

## Structure and Composition of Metal Substituted Calcium Deficient Hydroxyapatite

*E.P. Domashevskaya, A.A. Al-Zubadi, D.L. Goloshchapov,  
N.A. Rumyantseva and P.V. Seredin*

Voronezh State University, Voronezh, Russia, 394006 University Sq. 1

**Abstract:** Calcium hydroxyapatite (HAP)  $\text{Ca}_{10}(\text{PO}_4)_6(\text{OH})_2$  is an important material, which is applied in reconstruction of human solid tissue. In medicine, artificial materials based on HAP are used as ceramics and composites for recovering of bone and teeth and as implant coatings for better integration of synthetic materials with hydroxyapatite of human solid tissue. Phase and elemental composition of HAP samples by XRD and EPMA data has shown that under certain conditions method of chemical precipitation from solution calcium-deficient hydroxyapatite CDHAP could be produced with the calcium to phosphorous ratio  $\text{Ca/P} = 1.43$ . XRD analysis proved that all of the samples consist of nanocrystals with the average size of  $\sim 50$  nm. The obtained data show that the calcium deficiency in the crystal lattice of HAP is kept when calcium atoms are substituted by of Zn and Cu atoms. Partial substitution of calcium by Zn and Cu atoms of the radii less then calcium radius leads to the decrease of HAP cell unit parameters and reducing of nanocrystals average size.

**Key words:** Hydroxyapatite • Zn-HAP • Cu-HAP • Ca-deficient HAP • Nanocrystals • Phase composition

### INTRODUCTION

Calcium hydroxyapatite (HAP)  $\text{Ca}_{10}(\text{PO}_4)_6(\text{OH})_2$  is an important material, which is applied in reconstruction of human solid tissue. In medicine, artificial materials based on HAP are used as ceramics and composites for recovering of bone and teeth and as implant coatings for better integration of synthetic materials with hydroxyapatite of human solid tissue [1-5]. Depending on the type of bone and human individual characteristics in orthopedics different HAP-based materials with various properties are required. HAP characteristics variations can be obtained by including in HAP structure of different impurities in the cationic and anionic sublattices. According to these goals calcium-deficient hydroxyapatite (CDHAP) is the best in this case because of its structure and high chemical activity. Currently, this material is often used to restore human bones.

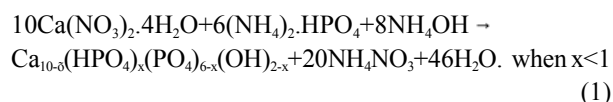
It is known that metal ions (Na, Mg, Zn, Cu, Fe, Sr), incorporated in the hydroxyapatite tier of bone tissue plays an important role in osteogenesis and affect the properties of biogenic HAP [6-7]. Deliberate injection of metal ions in synthetic hydroxyapatite lattice can lead,

besides better biocompatibility, to the changes in structural properties of these materials [7]. Among other impurities zinc and copper are actively also involved in process of ontogenesis. Zinc is present in the dental enamel and bone tissue increasing the activity of osteoblasts and plays an important role in the human immune system [7-8]. Copper ions just as silver ions have an antibacterial effect and in small concentrations facilitate an antiseptic effect on the affected area of bone [9]. All of the above mentioned metals provide the improvement of HAP bioactive properties. Articles devoted to this subject, indicate the possibility of obtaining such materials by chemical precipitation method [6,7,10] and describe the properties of copper and zinc-substituted HAP in comparison with other calcium phosphates. However, the problems concerned with the study of the structure and physicochemical properties of modified hydroxyapatite depending on the concentration of dopants and their influence on the phase composition of HAP have been studied rather incompletely.

The aim of this work is to determine the influence of metal ions  $\text{Zn}^{+2}$  and  $\text{Cu}^{+2}$  on the phase composition and structure of calcium-deficient hydroxyapatite.

## MATERIALS AND METHODS

Calcium-deficient hydroxyapatite (CDHAP) was prepared by chemical precipitation route [9, 11, 12]. The solution of 0,3 M  $(\text{NH}_4)_2\text{HPO}_4$  was added to the solution of 0,5 M  $\text{Ca}(\text{NO}_3)_2 \cdot 4\text{H}_2\text{O}$  dropwise and pH was adjusted to 9.5 by adding of 25% ammonia solution  $\text{NH}_4(\text{OH})$  until a white suspension was obtained according to the reaction (1):



The samples synthesis was monitored by measuring of pH values during the reaction using pH-meter/ionometer IPL-111-1 by "Multitest" as well as acid addition rate to the solution and also by the stirring rate. After 24 hours the samples were filtered, washed with distilled water and annealed at 400°C for 1 hour. The annealing temperature is conforming to the maximum vacancies content in the cation sublattice of CDHAP [12].

Copper- and zinc-substituted HAP (MeHAP) were prepared in the same process (1) with addition of 3 M metal salts solutions  $\text{Cu}(\text{NO}_3)_2 \cdot 3\text{H}_2\text{O}$  and  $\text{Zn}(\text{NO}_3)_2 \cdot 4\text{H}_2\text{O}$ . In both cases pH = 10.5 was attained by adding of 25% solution of  $\text{NH}_4(\text{OH})$  [13].

X-ray Diffraction (XRD) was studied with DRON 4-07 using  $\text{Co K}\alpha$ -radiation ( $\lambda = 1,7902 \text{ \AA}$ ) in the angular range  $10^\circ - 90^\circ$  in  $0.1^\circ$  steps under applied voltage of 20 kV and current of 10 mA. X-ray analysis was carried out using a database of ICDD (International Center for Diffraction Data).

The crystallite size was calculated by X-ray line broadening of the (002) reflex using Debye-Scherrer's equation (2).

$$D = k\lambda / \beta_{1/2} \cos\theta \quad (2)$$

where D is crystallite size, k- is a shape factor equal 0.9,  $\lambda$  - is wave length ( $\text{CoK}\alpha = 1,7902 \text{ \AA}$ ),  $\theta$  - is the diffraction angle related to 002 reflection ( $\theta = 30,16$ ) and  $\beta_{1/2}$ - is a difference between half width of the measured line and reference line.

The presence of changes in the bonds between the elements of the cation and anion sublattices CDHAP and Me-HAP was controlled by Fourier transform infrared spectroscopy. Registration of IR spectra was performed with VERTEX-70 produced by «Bruker» company, within the frequency range from 400 to  $4000 \text{ cm}^{-1}$ .

Determination of the elemental composition of the obtained CDHAP Me-HAP was conducted by the electron probe microanalysis (EPMA) with the X-ray microanalyzer JED-2200 attachment for the scanning electron microscope JEOL JSM 6610 A, which was also applied for the studies of the samples morphology.

## RESULTS AND DISCUSSION

**Phase Composition of the Samples:** Fig. 1 shows X-ray diffraction pattern for the undoped sample. According to the results of X-ray analysis in comparison with the card No 9-432 from the database JCPDS ICDD [14], it was found that the sample comprises a single phase of calcium hydroxyapatite (Table 1).

Fig. 2 shows X-ray diffraction patterns of zinc-substituted HAP (Zn-HA) samples with different concentrations of zinc 1,2,3% (curves 2, 3, 4) obtained at pH ~ 10 and annealed at 400°C. Comparison with undoped HAP sample (curve 1) revealed that all samples of zinc-substituted HAP represent substitutional solid solution based on hydroxyapatite. However, comparing the diffraction patterns concludes that with increasing concentration of Zn in the HAP diffraction lines are broadened, leading to a change in the shape of the most intensive reflection (211) (112). This may be related to the presence of lattice distortions in zinc-substituted HAP samples and with a decrease of the size of nanocrystals.

Fig. 3 shows X-ray diffraction patterns of copper - substituted HAP (Cu- HAP ) samples with copper concentrations Cu 1,2,3% ( curves 2, 3, 4 ) obtained at pH ~ 10 and annealed at 400C and undoped hydroxyapatite (curve1).

According to the results of X-ray analysis, it was found that the Cu- HAP samples (1%) (curve 2) and Cu- HAP (2%) (curve 3) comprise a single phase - calcium hydroxyapatite. Meanwhile, in the sample obtained with a higher content of copper Cu- HAP (3%) ( curve 4) low-intensity additional lines of the second phase  $\text{Ca}_{10}\text{Cu}_2\text{H}_2(\text{PO}_4)_{14}$  are detected (card No 46 -0412 [ 15]) along with the main phase HAP. The lines of this phase are marked in bold in Table 1.

Thus, the results of X-ray analysis show that applying the liquid phase method it is impossible to obtain single-phase HAP samples at the copper concentration exceeding 2% without some additional affects to the system. The reason for this difference in the behavior of Zn and Cu under replacing of calcium atoms in the HAP lattice can be explained by a significant

Table 1: Interplanar distances and relative intensities of the diffraction lines for synthesized CDHAP, Me-HAP with the substitution of Zn and Cu metals and reference HAP according to JCPDS-ICDD

No	Hydroxyapatite No 9-432 ICDD 1995			HAP		3% Zn/ HAP		3% Cu/ HAP	
	d	I	hkl	d	I	d	I	d	I
1	3.440	40	002	3.440	53	3.438	40	3.433	33.5
2	-	-	-	-	-	-	-	3.347	5
3	3.170	12	102	3.171	17	3.110	9	3.166	14
4	3.080	18	210	3.086	18	3.075	21.5	3.080	19.5
5	-	-	-	-	-	-	-	2.910	10
6	2.814	100	211	2.813	100	2.801	100	2.804	100
7	2.778	60	112	2.779	70	2.770	53		
8	2.720	60	300	2.725	43			2.721	44
9	2.631	25	202	2.630	24.5	2.625	20	2.629	34
10	2.528	6	301	2.526	16	2.520	5.1	2.524	8.5
11	2.296	8	212	2.310	18				
12	2.262	20	310	2.266	21.9	2.263	16.2	2.263	18.5
13	2.228	2	221						
14	2.148	10	311	2.152	14.5	2.150	3.4	2.143	18
15	2.134	4	302						
16	2.065	8	113	2.062	3.8	2.060	6.6	2.060	8
17	2.040	2	400						
18	2.000	6	203	1.999	12	1.999	3.2	1.999	7
19	1.943	30	222	1.943	20.5	1.946	56	1.938	22.5
20	1.890	16	312	1.890	17.5	1.899	15	1.893	
21	1.871	6	320						
22	1.841	40	213	1.840	24.5	1.840	60	1.839	44
23	1.806	20	321						
24	1.780	12	410						
25	1.754	16	402	1.753	3.5			1.750	18.5
26	1.722	20	004	1.722	18	1.720	20.5	1.716	16
27	1.684	4	104					1.683	4
28	1.644	10	322	1.646	13			1.645	10
29	1.611	8	313	1.619	2.1			1.611	9.5
30	1.587	4	501	1.586	1.8				
31	1.542	6	420					1.542	7
32	1.530	6	331	1.532	1.9				
33	1.503	10	214	1.500	2.3			1.504	8.5
34	1.474	12	502						
35	1.465	4	510						
36	1.452	13	304	1.450	18.5	1.448	13.5	1.454	10.5

difference in their electronic structure. Atomic structure of copper  $Cu\ 3d^{10}4s^1$  allows one to have as the divalent state in  $Ca_{10-x}Cu_x(PO_4)_6(OH)_2$  phase as monovalent state in  $Ca_{10}Cu_2H_2(PO_4)_{14}$  phase.

Table 1 shows the interplanar distances and intensity of the diffraction lines for the samples of CDHAP and MeHAP with the maximum concentration of metals (3%). From a comparison of the interplanar distances and intensities of the obtained samples with the corresponding values of the HAP sample from the database ICDD (card 9-432) it follows that CDHAP interplanar distances are in good agreement with the

corresponding values of the reference sample in the international database. At the same time for MeHAP samples one can observe the tendency in decreasing of interplanar distances compared to the sample No 9-432. Such a decrease is due to the substitution of Ca atoms with rather large radius of 1,95 Å by smaller atoms Zn (atomic radius 1,34 Å) and Cu (atomic radius 1,27 Å).

The lattice parameters for all hydroxyapatite samples were determined according to the "quadratic" formula for the hexagonal system (3): indices (310) for the parameter  $a$  and the indices (002) for the parameter  $c$ :

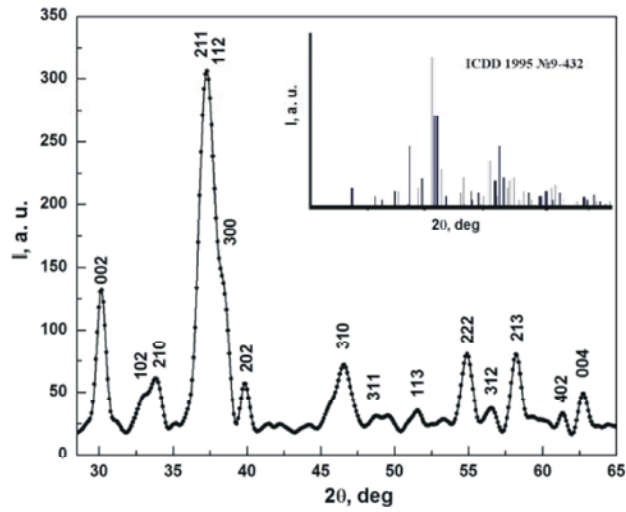


Fig. 1: XRD pattern of the undoped HAP sample prepared at pH = 9.5 and annealed at 400°C

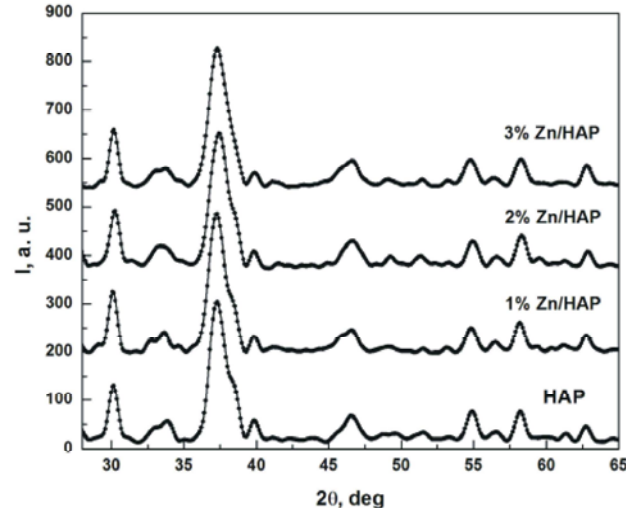


Fig. 2: XRD pattern of Zn-HAP 1% (curve 2), Zn-HAP 2% (curve 3), Zn-HAP 3% (curve 4) obtained at pH ~ 10 and annealed at 400°C and undoped HAP (curve 1)

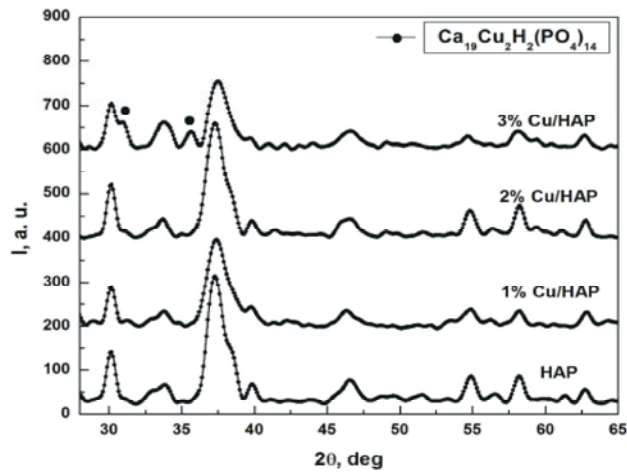


Fig. 3: XRD pattern of Cu-HAP 1% (curve 2), Cu 2% HAP (line 3), Cu-HAP 3% (curve 4) obtained at pH ~ 10 and annealed at 400C and undoped HAP (curve 1)

$$1/d^2 = (h^2 + hk + k^2)/a^2 + l^2/c^2 \quad (3)$$

The calculations showed that the parameters of  $a = 0.9434$  (nm) and  $c = 0.6880$  (nm) for undoped HAP agree well with the parameters of the reference sample in the international database (No 09-0432:  $a = 0.9418$  nm,  $c = 0.6884$  nm). At the same time the partial substitution of calcium atoms by smaller zinc and copper atoms leads to a certain decrease in the lattice parameters of HAP doped samples (Table 2). A similar effect was noted in [16].

**Evaluation of the Size of Crystallite:** Evaluation of the crystallite sizes of the samples was performed in accordance with the Debye-Scherrer formula (2), comparing the half width of the diffraction line (002) for the investigated samples ( $2\theta = 25.97$  ( $6^\circ$ )), with half the width of (111) line of polycrystalline silicon ( $2\theta = 28.512^\circ$ ). Table 3 shows the measured values of half the width of the diffraction line (002) and the calculated sizes of the nanocrystals of all the prepared samples.

The results show that by precipitation from solution we obtained undoped nanocrystalline hydroxyapatite with nanocrystal sizes of  $\sim 50$  nm, comparable to the size of nanocrystals obtained by similar methods in the other studies [17-20]. The comparison of the crystallite sizes in CDHAP and MeHAP indicates (Table 3) that the incorporation of Zn and Cu metals into the crystalline lattice of HAP leads to some decrease in the sizes of nanocrystals.

**Elemental Composition of the Obtained Samples:** Determination of the elemental composition and stoichiometry of the obtained materials was made by microanalysis (EPMA) method. The results of EPMA for CDHAP and Me-HAP samples with a maximum content of metals is shown in Table 4.

The results of EPMA show that in undoped hydroxyapatite sample Ca/P ratio is equal to 1.43 which is significantly lower than the stoichiometric one (1.67). This fact confirms that we produced calcium-deficient hydroxyapatite CDHAP. The presence of Zn in HAP crystal lattice does not almost change Ca/P ratio, while Cu reduces this value.

**Results of IR Spectroscopy:** To determine the possible changes in the bonds between the elements in the cation and anion sublattices of CDHAP and Me-HAP samples IR spectra were obtained. Figures 4 and 5 show the IR spectra of zinc-substituted and copper-substituted HAP in comparison of IR spectrum of undoped HAP.

Table 2: Parameters of the crystal lattice and unit cell volumes of the samples

Sample	$a$ (nm)	$c$ (nm)	$V(\text{nm})^3$
CDHAP	0.9434	0.6880	0.5313
1% Zn-HAP	0.9429	0.6878	0.5295
2% Zn-HAP	0.9425	0.6876	0.5289
3% Zn-HAP	0.9421	0.6876	0.5285
1% Cu-HAP	0.9434	0.6878	0.5301
2% Cu-HAP	0.9429	0.6876	0.5294
3% Cu-HAP	0.9421	0.6866	0.5277

Table 3: Half width of the (002) line and the crystallite sizes in CDHAP and Me-HAP samples

Sample	(002) Half width ( $^\circ$ )	Crystallite size D(nm)
CDHAP	0.388	54
1% Zn-HAP	0.390	50
2% Zn-HAP	0.470	38
3% Zn-HAP	0.495	35
1% Cu-HAP	0.430	45
2% Cu-HAP	0.447	42
3% Cu-HAP	0.420	47

Table 4: Elemental composition and the value of Ca / P ratio for the samples CDHAP and Me-HAP (3%)

El	HAP	Zn- HAP 3%	Cu- HAP 3%
Ca	24,22	24,09	22,74
O	58,87	59,10	59,13
P	16,91	16,51	18,08
Zn	---	0,3	---
Cu	---	---	0,05
Ca/P	1,43	1,46	1,26

Identification of the vibration modes in IR spectra of the samples was performed using the known literature data [12,21], whereby it was found that the spectra of the studied materials involve vibration modes specific to the HAP. Frequencies of the vibration modes in the obtained samples, together with the known literature data presented in Table 5.

The results show that two high-intensity groups of vibrations at  $1090-960\text{ cm}^{-1}$  and  $600-560\text{ cm}^{-1}$  are related to  $\text{PO}_4^{3-}$  complex. Vibration modes observed at  $3572$  and  $630\text{ cm}^{-1}$  correspond to OH<sup>-</sup> group. In addition, in the spectra of all samples the low-intensity modes  $880$  and  $725\text{ cm}^{-1}$  are found, related belonging to the groups  $\text{HPO}_4^{2-}$  and  $\text{P}_2\text{O}_7^{4-}$ . The latter confirms the nature of the calcium - deficient hydroxyapatite in all the obtained samples as undoped HAP as MeHAP [22].



**Study of Morphology:** Morphological features of undoped and metal calcium deficient hydroxyapatite samples were investigated by SEM. The results are shown

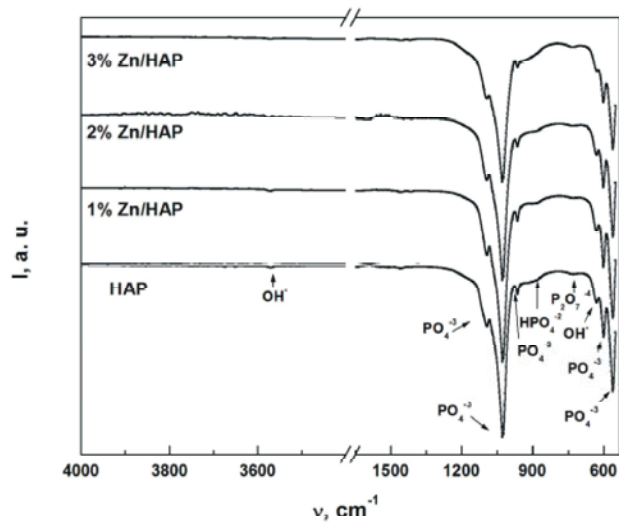


Fig. 4: IR-spectra of the samples 1% Zn-HAP (curve 2), 2% Zn-HAP (curve 3), 3% Zn-HAP (curve 4) obtained at pH ~ 10 and annealed at 400°C and undoped HAP (curve 1)

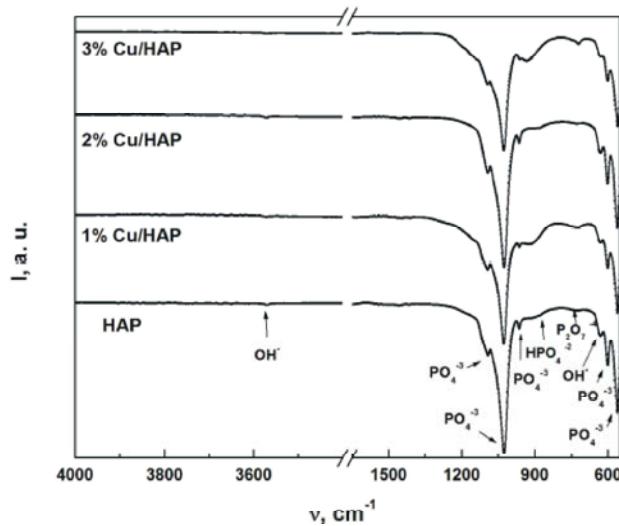


Fig. 5: IR spectra of samples 1%Cu-HAP (curve 2), 2%Cu-HAP (curve 3), 3%Cu-HAP (curve 4) obtained at pH ~ 10 and annealed at 400°C and undoped CDHAP (curve 1)

Table 5: Vibration modes of the infrared spectra (IR) of samples CDHAP and Me-HAP

Vibration modes	Vibrational frequencies $\nu$ $\text{cm}^{-1}$							The published data	
	Experimental data								
	HAP	1% Zn- HAP	2% Zn- HAP	3% Zn- HAP	1% Cu- HAP	2% Cu- HAP	3% Cu- HAP	CDHAP [12]	HAP [21]
$\text{PO}_4^{3-}$ ( $\nu^4$ )	568	565	560	564	561	560	560	565	565
$\text{PO}_4^{3-}$ ( $\nu^4$ )	599	601	600	600	599	603	599	602	602
$\text{OH}^-$	627	628	628	628	629	632	632	-	630
$\text{P}_2\text{O}_7^{4-}$	725	724	727	722	720	720	725	725	-
$\text{HPO}_4^{2-}$	880	875	877	873	880	876	874	875	-
$\text{PO}_4^{3-}$ ( $\nu^1$ )	960	965	965	965	960	963	961	962	964
$\text{PO}_4^{3-}$ ( $\nu^3$ )	1019	1024	1024	1024	1025	1023	1028	1032	1041
$\text{PO}_4^{3-}$ ( $\nu^3$ )	1087	1095	1090	1097	1090	1091	1092	1093	1095
$\text{OH}^-$	3570	3575	3573	3570	3574	3572	3566	3570	3570

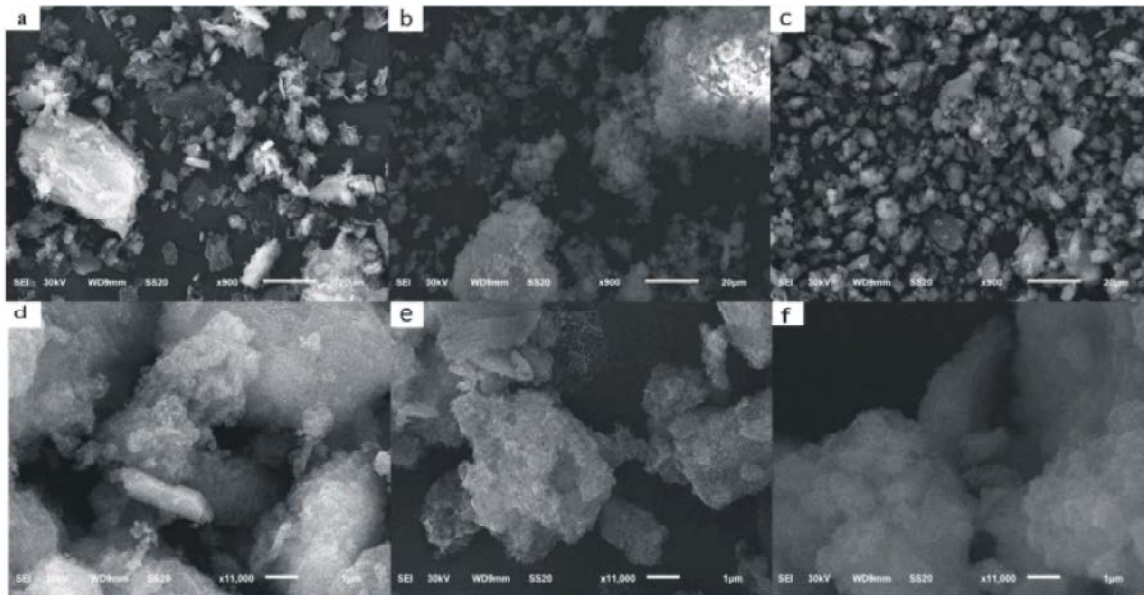


Fig. 6: SEM data of morphological features of undoped and metal calcium deficient hydroxyapatite samples. X900 a) undoped CDHAP,  $\alpha$ ) 3% Zn-HAP,  $\beta$ ) 3%Cu-HAP. X11000  $\gamma$ ) undoped CDHAP,  $\lambda$ ) 3% Zn-HAP,  $\mu$ )3%Cu-HAP

in Figure 6. With an increase of 900 times is observed for all samples the presence of large globules of different sizes. In unalloyed sample CDHAP agglomerate size varies in the widest range of 1 to 40 microns (Figure 6a), whereas in Cu- HAP agglomerate size is reduced to an average of 20 microns (Fig. 6 b,c). Scaled up to x11000 discover complex structure of the agglomerates. According to the X-ray analysis, these agglomerates are comprised of a variety of nanocrystals with the average dimensions of about 50 nm.

### CONCLUSION

The results of complex investigations of the phase and elemental composition for HAP samples have shown that under certain conditions method of chemical precipitation from solution calcium-deficient hydroxyapatite CDHAP could be produced with the calcium to phosphorous ratio  $Ca/P = 1.43$ .

By means of the XRD analysis it was proved that all of the samples consist of nanocrystals with the average size of  $\sim 50$  nm.

The obtained data shows that the calcium deficiency in the crystal lattice of HAP is kept when calcium atoms are substituted by of Zn and Cu atoms.

Partial substitution of calcium by Zn and Cu atoms of the radii less than that of calcium leads to the decrease in HAP cell unit parameters and reduction of nanocrystals average size.

Increase of copper content in Cu-HAP up to 3% results in the second phase  $\tilde{N}a_{19}Cu_2H_2(PO_4)_{14}$  with monovalent copper.

### ACKNOWLEDGEMENTS

The work was supported by Russian Science Foundation.

### REFERENCES

1. Wiria, F.E., B.Y. Tay, P.N. Lim and E. Ghassemieh, 2010. "Porosity and cell culture investigation of hydroxyapatite component for biomedical application," SIM Tech, 11(1): 6-10.
2. Velisavljevic, N. and K. Yogesh, Vohra, 2003. "Bioceramic hydroxyapatite at high pressures," Applied Physics Letters, 82(24): 4271-4273.
3. Markovic, M., O. Fowler and S. Ming Tung, 2004. "Preparation and Comprehensive Characterization of a Calcium Hydroxyapatite Reference Material," Journal of Research of the National Institute of Standards and Technology, 109(6): 553-568.
4. Li, C., J. Liang, J. Niu, S. Liu, G. Li, J. Bai, A. Zhang, R. Ding, 2011. "Characterization of hollow hydroxyapatite copper microspheres prepared from the reduction of copper modified hydroxyapatite by glucose," Electron Microscop, 60: 301-305.

5. Danilchenko, C.N., 2007. "Morphology and structure of biogenic apatite crystals according to transmission electron microscopy and electron diffraction," *Series Physics*, 2: 94-100.
6. Krzysztof Szostek, Henryk Glab, 2011. " Trace elements concentrations in human teeth from a neolithic common grave at Nakonowo," 9: 51-59.
7. Thian, E.S., T. Konishi and Y. Kawanobe, 2013. "Zinc-substituted hydroxyapatite: a biomaterial with enhanced bioactivity and antibacterial properties," *Mater Sci: Mater Med*, 24: 437-445.
8. Norhidayu, D., I. Sopyan and S. Ramesh, 2008. "Development of Zinc Doped Hydroxyapatite for Bone Implant Applications," *of the American Ceramic Society*, 89(9): 257-270.
9. Hui Yang, Bingjuan Xiao, Ke-Wei Xu, 2009. "Synthesis and characterization of Ag/Cu/HAP with platelet morphology," *Mater Sci: Mater Med*, 20(3): 785-792.
10. Gross, K.A., L. Komarovska and A. Viksna, 2013. "Efficient zinc incorporation in hydroxyapatite through crystallization of an amorphous phase could extend the properties of zinc apatites," *of The Australian Ceramic Society*, 49(2): 129-135.
11. Devanand Venkatasubbu, G. and S. Ramasamy, 2011. "Nanocrystalline hydroxyapatite and zinc-doped hydroxyapatite as carrier material for controlled delivery of ciprofloxacin," *Biotech*, 3: 173-186.
12. Siddharthan, A., S. K. Seshadri and T.S. Sampath Kumar, 2005. "Rapid Synthesis of Calcium Deficient Hydroxyapatite Nanoparticles by Microwave Irradiation," *Trends Biomater*, 18(2): 110-112.
13. Riad, M. and S. Mikhail, 2010. " Zinc Incorporated Hydroxyapatite as Catalysts for Oxidative Desulphurization Process," *Researches in Engineering*, 10(1): 85-91.
14. JCPDS -ICDD 1995 Card No 9-432.
15. JCPDS -ICDD 2001 Card No 46-0412.
16. ElMhammedi, M.A., M. Achak and H. Massa, 2010. "Preparation and physicochemical characterization of hydroxyapatite coatings on zinc surfaces," *J. Coat. Technol. Res.*, 7(6): 715-720.
17. Devanand Venkatasubbu, G. and S. Ramasamy, 2011. "Investigations on Zinc Doped nanocrystalline hydroxyapatite," *International Journal of Nanoscience and Nanotechnology*, 2(1): 1-23.
18. Dan Nicolae Ungureanu, Nicolae Angelescu and Zorica Bacinschi, 2011. "Thermal stability of chemically precipitated hydroxyapatite nanopowders," *International Journal Of Biology And Biomedical Engineering*, 5(2): 57-62.
19. Kashkarov, V.M., D.L. Goloshapov, A.N. Rumyantseva, P.V. Seredin, E.P. Domashevskaya and I.A. Spivakova, 2011. "X-Ray Diffraction and IR Spectroscopy Investigation of Synthesized and Biogenic Nanocrystalline Hydroxyapatite," *Journal of Surface Investigation. X- ray, Synchrotron and Neutron Techniques*, 5(6): 1162-1167.
20. Ingrid Russoni De Lima and Andrea Machado Costa, 2006. "Development and Characterization of 5% mol Zn Bioceramic in Granular Form," *Materials Research*, 9(4): 399-403.
21. Liga Berzina Cimdina, Natalija Borodajenko, 2012. "Research of Calcium Phosphates Using Fourier Transform Infrared Spectroscopy," *Journal: Infrared Spectroscopy –Materials Science, Engineering and Technology*, pp: 123-148.
22. Tamai, M., M. Nakamura, T. Isshiki, K. Nishio, H. Endoh and A. Nakahira, 2003. "A metastable phase in thermal decomposition of Ca-deficient hydroxyapatite," *Journal of Materials Science: Materials in Medicine*, 14(7): 617-622.